IEEE Access
Multidisciplinary | Rapid Review | Open Access Journal

Received February 9, 2020, accepted March 5, 2020, date of publication March 10, 2020, date of current version March 26, 2020.

Digital Object Identifier 10.1109/ACCESS.2020.2979757

High Precision Tri-Axial Quartz Flexible Accelerometers Resolution Measurement Method Based on Tri-Axial Turntable

CHUNXI ZHANG[1], MINPENG DAI[1], WEI LUO[2], AND XIONG PAN[1]
[1]School of Instrumentation Science and Optoelectronics Engineering, Beihang University, Beijing 100191, China
[2]9th Designing of China Aerospace Science Industry Corporation, Wuhan 430000, China

Corresponding author: Xiong Pan (08768@buaa.edu.cn)

ABSTRACT Aiming at the high requirements of the experimental equipment for the measurement of high precision quartz flexible accelerometer resolution, the gravity measured by high precision tri-axial accelerometers was subdivided by the tri-axial turntable. Tri-axial quartz flexible accelerometers resolution measurement model was established and general mathematical expression for the resolution measurement was derived. Based on the mathematical expression, the effective angle range that satisfied the measurement condition was given out. Besides, the tri-axial quartz flexible accelerometers resolution measurement process was designed. Within the effective angle range, numerical simulations were performed and the simulation results showed that: the proposed method can theoretically measure tri-axial quartz flexible accelerometers of which the resolution was about 10^{-6}g. Then the tri-axial quartz flexible accelerometers resolution repetitive measurement experiments were carried out and the experimental results illustrated that: the difference between the measured value with the theoretical value is within 1μg, which met the requirements for use. In addition, the resolution of tri-axial quartz flexible accelerometers can be measured at one time based on the designed process, demonstrating that the proposed method was valid.

INDEX TERMS Tri-axial turntable, tri-axial quartz flexible accelerometers, gravity subdivision, resolution measurement.

I. INTRODUCTION

High precision tri-axial quartz flexible accelerometers are a decisive component of high accuracy gravity measurement system, and also play an important part of high precision inertial navigation equipment [1]. Through the specific force information of the carrier provided by the tri-axial quartz flexible accelerometers, the gravity measurement system can complete the measurement of the gravity vector of the surrounding environment, and the inertial navigation device can achieve accurate guidance. The tri-axial quartz flexible accelerometers must be calibrated and measured before use to compensate for sensor errors. As the precision of gravity measurement systems and inertial navigation equipment continue to improve, higher requirements have been put forward for tri-axial quartz flexible accelerometer performance measurement [2]–[4].

Many scholars have studied the measurement method of high precision tri-axial quartz flexible accelerometers systems and representative works include: Li *et al.* calibrated the bias and scale factor of inertial measurement unit (IMU) in a short time using Kalman filter combined with navigation algorithms of coupled global position system/inertial navigation system (GPS/INS) integrated systems [5]. Chang *et al.* designed a system-level sway calibration scheme to make full use of the sway motion caused by sea waves and calibrated the system parameters of the inertial device in real time [6]. Cao *et al.* proposed a system-level continuous self-calibration scheme for a new type of tri-axial rotary modulation inertial measurement device. By alternately processing the step of multiple positions and continuous rotation, it suppressed dynamic errors and enhanced system error parameter excitation [7]. Klimkovich put forward a system-level strapdown inertial navigation system (SINS) calibration method using IMU error equation at any rotation rate to estimate gyroscope and accelerometer errors by Kalman filter [8]. Qureshi *et al.* came up with a low-cost IMU calibration method that used gravity signals as a stable reference without external equipment. It used the least square method and applied simple

The associate editor coordinating the review of this manuscript and approving it for publication was Jenny Mahoney.

rotation to provide relatively easy and fast calibration [9]. Li *et al.* proposed a fast discrete calibration method for horizontal drilling platforms, and illustrated five rapid horizontal calibration schemes for the main errors of measuring-while-drilling inertial measurement unit (MWD-IMU) [10]. Song *et al.* proposed a discrete calibration method for calibrating the installation error between the IMU and the turntable in a dual axes modulation inertial navigation system [11]. All of the above are related to measuring at the system-level. The representative tasks of device-level measurement include: Ranjbaran *et al.* proposed a new variable change method to convert the nonlinear optimization problem into linear least squares (LLS) equation. The bias, scale factor and axis misalignment of the accelerometer can be estimated [12]. Liu *et al.* put forward an accelerometer bias estimation method without a turntable and established a coupling model of gravity vector and accelerometer bias [13]. Won *et al.* used the sum of the output of the tri-axial accelerometers is equal to the gravity vector to calibrate the bias and scale factor [14]. Guan *et al.* made use of a dual-turntable centrifuge as a device that provides standard acceleration reference to calibrate the lateral sensitivity of the low-frequency accelerometer [15]. Wu *et al.* took advantages of the precise angle of the space-stabilized platform and realized the self-calibration of a three-stage accelerometer in spatially stable INS [16]. Yu *et al.* proposed a method for continuously adjusting the accelerometer's scale factor and installation error to reduce motion sensitivity. Based on the analysis model of the rotational accelerometer gravity gradient meter (RAGG), a compensation signal was generated to compensate the motion error [17]. Bezděk *et al.* calibrated the accelerometer based on the observed GPS position and verified the accuracy of the calibration by three different methods [18]. As we can see, the calibration draws much attention and oceans of researches have been done. Meanwhile, the resolution of accelerometer also contributes to the precision of gravity measurement systems and inertial navigation equipment. Some typical work is carried out as follows: Ma *et al.* exploited the dual-axial turntable to subdivide the gravity and achieved the measurement of an accelerometer of which the resolution is about 10^{-8}g [19]. Wu *et al.* came up with an accelerometer resolution measurement method based on the dual-axial tilt method, and the specific implementation process and examples were given. Measurement and analysis proved that the method can detect accelerometer resolution below 1μg [20]. They only used the dual-axial turntable to measure single axis accelerometer resolution at several special points, which was equivalent to a special measurement case. And the general effective angle range satisfied the measurement requirements has not been studied in depth and given out. Li *et al.* presented a dynamic resolution estimation method of using dual-axial turntable. The output of accelerometer was sampled, and the data was filtered by the FFT low-pass filter. The resolution of accelerometer may be determined by analyzing the maximum change at the peak and valley value. It combines the equipment and algorithm, which seems complex and the mathematical express of the resolution is unclear [21]. The traditional accelerometer resolution measurement is generally performed on a precision crown wheel or precision optical dividing head. The accelerometer is mounted on the dividing head table through a fixture so that the input axis of the accelerometer is parallel to the table. The input axis of the accelerometer is rotated in the vertical plane relative to gravity. By measuring the angle between the sensitive axis and the gravity vector, the acceleration value can be calculated. However, this method must adopt vibration isolation and anti-tilt measures [22]. Hu *et al.* still used the dividing head for testing, but in the conventional test, the input axis of the accelerometer was tested near the plumb line instead of the horizon, which greatly reduced the sensitivity of the change of the gravity acceleration component of the input axis of the accelerometer to the rotation angle of the dividing head, thus significantly reducing the impact of the accuracy of the dividing head on the test results. But it is just a little improve based on the traditional method and detailed analysis is not given out [23].

In view of the above situation, this paper proposes a high precision tri-axial accelerometers resolution measurement method based on a tri-axial turntable. A general mathematical expression for resolution measurement is given out and. The effective angle range that meets the resolution measurement requirements is calculated and the process of the tri-axial accelerometers resolution measurement is designed. The main contributions of this paper are as follows:

(1) the tri-axial accelerometers resolution measurement model was established and general mathematical expression for the resolution measurement was derived. Based on the mathematical expression, the effective angle range that satisfied the measurement conditions was given out;

(2) the tri-axial accelerometers resolution measurement process was designed. The resolution of three axes can be measured at one time based on the designed process.

The chapters of this article are arranged as follows: section I is an introduction; section II discusses the proposed method; mathematical simulation and analysis are carried out in section III; experiments are conducted in section IV; conclusions are drawn in section V.

II. HIGH PRECISION TRI-AXIAL QUARTZ FLEXIBLE ACCELEROMETERS RESOLUTION MEASUREMENT METHOD BASED ON TRI-AXIAL TURNTABLE

A. RESEARCH OBJECT

The research object of this paper is a tri-axial orthogonal quartz flexible accelerometers, which consists of three single-degree-of-freedom accelerometers. They are perpendicular to each other and the schematic diagram is shown in Figure 1:

It can be seen from Figure 1 that the x-axis, y-axis and z-axis of the tri-axial orthogonal accelerometers are perpendicular to each other, which are sensitive to the specific force information in three directions respectively. The installation

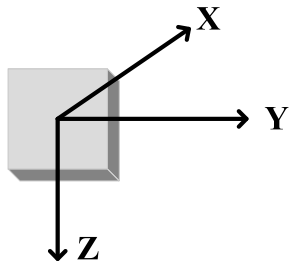

FIGURE 1. The schematic diagram of tri-axial accelerometers.

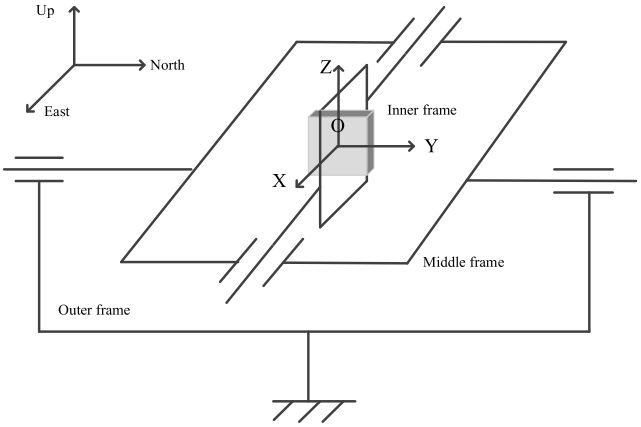

FIGURE 2. The installation diagram of the tri-axial turntable and the tri-axial accelerometers.

diagram of the tri-axial turntable and the tri-axial accelerometers is shown in Figure 2:

As is shown in Figure 2, the tri-axial accelerometers are installed in the inner frame of the tri-axial turntable, and the y-axis of the tri-axial accelerometers is parallel to the rotation axis of the middle frame, pointing to the north; the x-axis of the tri-axial accelerometers is parallel to the rotation axis of the inner frame, pointing to the East; the z-axis of the tri-axial accelerometers is parallel to the rotation axis of the outer frame, pointing to the sky. O_{xyz} is defined as the body system of tri-axial accelerometers, recorded as b-system. And navigation system is recorded as n-system.

B. MATHEMATICAL MODEL

Rotate the outer frame, inner frame, and middle frame of the tri-axial turntable by turns for an angle of γ, α and β, the transition matrix from n-system to b-system can be written as (1) shown at the bottom of the this page.

The measured gravity vector of tri-axial accelerometers can be expressed as (2), shown at the bottom of the this page, where g_{XA1} is the measured gravity vector of x-axis; g_{YA1} is the measured gravity vector of y-axis; g_{ZA1} is the measured gravity vector of z-axis. Simplify formula (2) to (3):

$$\begin{bmatrix} g_{XA1} \\ g_{YA1} \\ g_{ZA1} \end{bmatrix} = \begin{bmatrix} \sin\beta\cos\alpha \\ -\sin\alpha \\ -\cos\beta\cos\alpha \end{bmatrix} g \tag{3}$$

The relationship between the measured gravity vector of each axis and γ, α and β are obtained, as shown in (4), (5) and (6) respectively.

$$g_{XA1} = g\sin\beta\cos\alpha \tag{4}$$
$$g_{YA1} = -g\sin\alpha \tag{5}$$
$$g_{ZA1} = -g\cos\beta\cos\alpha \tag{6}$$

Taking this position as the initial position for resolution measurement, then rotate the outer frame, inner frame, and middle frame of the tri-axial turntable in turn for an angle of $\Delta\gamma$, $\Delta\alpha$ and $\Delta\beta$. So g_{XA}, g_{YA} and g_{ZA} are expressed as (7), (8) and (9) respectively, which are the general mathematical expression for the resolution measurement.

$$g_{X_4} = g(\sin(\beta+\Delta\beta)\cos(\alpha+\Delta\alpha) - \sin\beta\cos\alpha) \tag{7}$$
$$g_{YA} = (-\sin(\alpha+\Delta\alpha) + \sin\alpha)g \tag{8}$$
$$g_{ZA} = (-\cos(\beta+\Delta\beta)\cos(\alpha+\Delta\alpha) + \cos(\beta)\cos(\alpha)) \tag{9}$$

C. EFFECTIVE ANGLE RANGE SOLUTION

Let $\Delta\alpha = \Delta\beta = 2''$, compared to γ, α and β, $\Delta\gamma$, $\Delta\alpha$ and $\Delta\beta$ are tiny quantities so that g_{XA}, g_{YA} and g_{ZA} can be represented as (10), (11) and (12), where $d\alpha = d\beta = \Delta\alpha = \Delta\beta = 2''$.

$$dg_{XA} = g(\cos\beta\cos\alpha d\beta - \sin\beta\sin\alpha d\alpha) \tag{10}$$
$$dg_{YA} = -g\cos\alpha d\alpha \tag{11}$$
$$dg_{ZA} = g(\sin\beta\cos\alpha d\beta + \cos\beta\sin\alpha d\alpha) \tag{12}$$

The resolution of high precision tri-axial quartz flexible accelerometers is generally 10^{-6}g so that (13) shall be met to achieve the measurement.

$$\begin{cases} |dg_{XA}| = |g(\cos\beta\cos\alpha d\beta - \sin\beta\sin\alpha d\alpha)| \le 10^{-6}g \\ |dg_{YA}| = |-g\cos\alpha d\alpha| \le 10^{-6}g \\ |dg_{ZA}| = |g(\sin\beta\cos\alpha d\beta + \cos\beta\sin\alpha d\alpha)| \le 10^{-6}g \end{cases} \tag{13}$$

(14), (15) and (16) are obtained by simplifying (13):

$$|\beta+\alpha| \le \arccos(0.1) \tag{14}$$
$$|\alpha| \le \arccos(0.1) \tag{15}$$
$$|\beta+\alpha| \le \arcsin(0.1) \tag{16}$$

$$C_n^b = \begin{bmatrix} \cos\beta\cos\gamma - \sin\gamma\sin\alpha\sin\gamma & \cos\beta\sin\gamma + \sin\beta\sin\alpha\cos\gamma & -\sin\beta\cos\alpha \\ -\cos\alpha\sin\gamma & \cos\alpha\cos\gamma & \sin\alpha \\ \sin\beta\cos\gamma + \cos\beta\sin\alpha\sin\gamma & \sin\beta\sin\gamma - \cos\beta\sin\alpha\cos\gamma & \cos\beta\cos\alpha \end{bmatrix} \tag{1}$$

$$\begin{bmatrix} g_{XA1} \\ g_{YA1} \\ g_{ZA1} \end{bmatrix} = \begin{bmatrix} \cos\beta\cos\gamma - \sin\gamma\sin\alpha\sin\gamma & \cos\beta\sin\gamma + \sin\beta\sin\alpha\cos\gamma & -\sin\beta\cos\alpha \\ -\cos\alpha\sin\gamma & \cos\alpha\cos\gamma & \sin\alpha \\ \sin\beta\cos\gamma + \cos\beta\sin\alpha\sin\gamma & \sin\beta\sin\gamma - \cos\beta\sin\alpha\cos\gamma & \cos\beta\cos\alpha \end{bmatrix} \begin{bmatrix} 0 \\ 0 \\ -g \end{bmatrix} \tag{2}$$

(14), (15) and (16) are x-axis measurement requirement, y-axis measurement requirement and z-axis measurement requirement respectively. Analyzing (14), (15) and (16), it is obvious that x-axis and y-axis can be measured at the same time, x-axis and z-axis as well as y-axis and z-axis cannot be measured together. So at most, the resolution of two axes can be measured at one time, and these two axes are x-axis and y-axis. By solving equation (14) and (15), we can get (expressed in radian):

$$\begin{cases} 1.4706(+\pi) \le \alpha \le 1.6710(+\pi) \\ -0.002(+\pi) \le \beta \le 0.002(+\pi) \end{cases}$$
$$st\ |\alpha + \beta|\ \varepsilon\ [1.4706, 1.6710] + \pi \qquad (17)$$

(17) is the initial requirement that the resolution of x-axis and y-axis can be measured. Similarly, formula (18), which is the initial requirement of z-axis, can be obtained by solving (16):

$$-0.102(+\pi) \le |\alpha + \beta| \le 0.102(+\pi) \qquad (18)$$

D. TRI-AXIAL ACCELEROMETERS RESOLUTION MEASUREMENT PROCESS

According to the analysis in section C of chapter II, at most the resolution of two axes can be measured at one time. In order to measure the resolution of all axes together, following measurement process is proposed.

Resolution measurement process

Step1 : Turn on the three-axis turntable and collect data;

Step2 : Rotate the outer frame to 0 °position;

Step3: Rotate the inner frame to 0 ° position;

Step4: Rotate the middle frame to 90 ° position;

Step5: Rotate the inner frame and the middle frame for 2 arc seconds respectively;

Step6: Rotate the middle frame to 0 °position ;

Step7: Rotate the middle frame for 2 arc seconds;

Step8: Reset and turn off the three-axis turntable.

III. MATHEMATICAL SIMULATION

According to part C of section II, the resolution measurement requirements of x-axis and y-axis, named (17), are simulated. In this angle range, 10 groups of points are randomly selected. The theoretical measurable resolution results of x-axis and y-axis are shown in Table 1.

It can be seen from Table 1 that within the range specified in equation (17), the theoretical measurable resolution of x-axis and y-axis obtained by simulation are less than 10^{-6}g, which is consistent with the theoretical derivation.

In the same way, the resolution measurement requirement of z-axis, recorded as (18), is simulated. In this angle range, 10 groups of points are randomly selected, and the theoretical measurable resolution results of z-axis are shown in Table 2.

It can be seen from Table 2 that within the range specified in equation (18), the theoretical measurable resolution of z-axis obtained by simulation is less than 10^{-6}g, which is consistent with the theoretical derivation too. According to the simulation results, it is not difficult to see that in the range given in this paper, the absolute value measurement requirements of accelerometer resolution are met.

TABLE 1. Simulation results of theoretically measurable resolution of x-axis and y-axis.

Serial number	α (rad)	β (rad)	g_{XA} (g)	g_{YA} (g)
1	1.6710	-0.002	-9.5077×10^{-7}	9.7002×10^{-7}
2	1.6700	-0.001	-9.5121×10^{-7}	9.6038×10^{-7}
3	1.6690	0.001	-9.6042×10^{-7}	9.5073×10^{-7}
4	1.6680	0.0015	-9.5560×10^{-7}	9.4108×10^{-7}
5	1.6670	0.002	-9.5077×10^{-7}	9.3143×10^{-7}
6	1.4710	0.002	9.4666×10^{-7}	-9.6600×10^{-7}
7	1.4720	0.0015	9.4138×10^{-7}	-9.5635×10^{-7}
8	1.4730	0.001	9.3701×10^{-7}	-9.4670×10^{-7}
9	1.4740	-0.0015	9.5148×10^{-7}	-9.3705×10^{-7}
10	1.4750	0.0015	9.1287×10^{-7}	-9.2740×10^{-7}

TABLE 2. Simulation results of theoretically measurable resolution of x-axis and y-axis.

Serial number	α (rad)	β (rad)	g_{ZA} (g)
1	0.1	0.002	9.8740×10^{-7}
2	0.08	0.004	8.1362×10^{-7}
3	0.09	0.003	9.0055×10^{-7}
4	0.101	0.001	9.8740×10^{-7}
5	0.095	0.005	9.6811×10^{-7}
6	-0.1	-0.002	-9.8721×10^{-7}
7	-0.05	-0.045	-9.1967×10^{-7}
8	-0.06	-0.03	-8.7139×10^{-7}
9	-0.04	-0.06	-9.6792×10^{-7}
10	-0.07	-0.025	-9.1967×10^{-7}

IV. EXPERIMENTAL ANALYSIS

According to the simulation results in section III, a ground experiment for tri-axial accelerometers resolution measurement is designed to verify the correctness of the method in this paper. The IMU used in the experiment was a self-developed optical fiber IMU, and the resolution of the tri-axial accelerometers are about 10ug. The self-developed optical fiber IMU and the tri-axial turntable are installed with screws and adapter board, and the X, Y, and Z axes are pointing to east, north, and sky respectively, as shown in Figure 3.

The temperature in the experimental room is stabilized at about 25 ° C using an air conditioner for 2h before experiment. First, the x-axis and y-axis resolution measurement experiments are performed. Three points are randomly selected within the range of formula (17), and each point is repeated 3 times. First turn the turntable to the specified position. After the turntable is stable, rotate the frame corresponding to the axis to be measured for 2 arc seconds, and make a difference between the data before and after rotating the turntable. The results of the repeated experiments are shown in Figure 4.

As is shown in Figure 4, there is a tiny alteration in g_{XA} and g_{YA} with the rotation of turntable. The green short dash

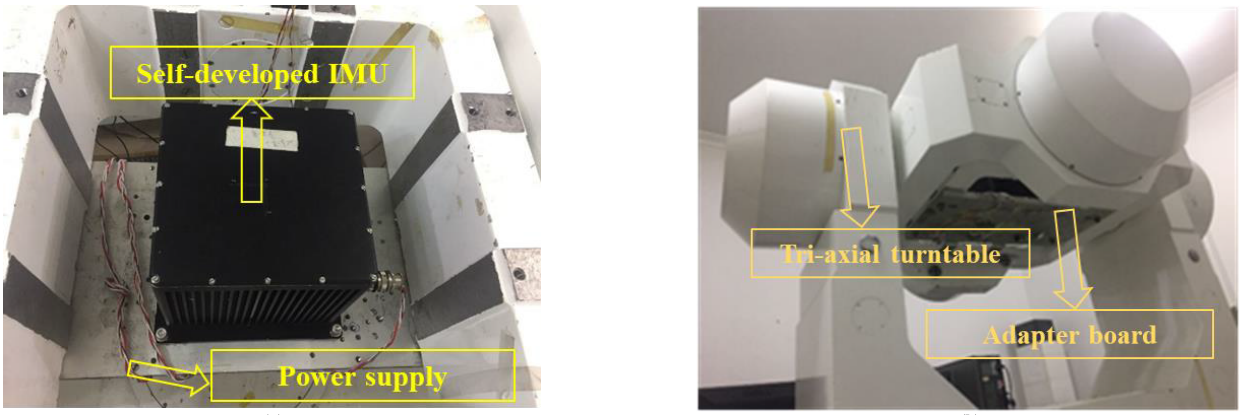

FIGURE 3. Ground verification experimental device.

TABLE 3. Results of three repeated experiments for resolution measurement of x-axis and y-axis.

Serial number	g_{XA}(unit:g) Before rotation	After rotation	Difference	g_{YA}(unit:g) Before rotation	After rotation	Difference
			α =1.5698 , β =0.0002			
1	0.002265	0.002254	0.000011	0.003229	0.003218	0.000011
2	0.002268	0.002257	0.000011	0.003233	0.003223	0.000011
3	0.002268	0.002258	0.00001	0.003230	0.003219	0.000011
			α =1.5708 , β =-0.0002			
1	0.002665	0.002655	0.00001	0.002352	0.002342	0.00001
2	0.002664	0.002653	0.000011	0.002352	0.002340	0.000012
3	0.002665	0.002655	0.00001	0.002352	0.002341	0.000011
			α =1.5716 , β =-0.001			
1	0.003452	0.003442	0.00001	0.001657	0.001647	0.00001
2	0.003453	0.003443	0.00001	0.001656	0.001647	0.000009
3	0.003453	0.003442	0.000011	0.001656	0.001646	0.00001

represents primary smoothing sequence. By contrast, the red line represents initial sequence's average value. From the red line, we can easily calculate out the resolution. The value of g_{XA} and g_{YA} are list in Table 3.

According to Table 3, the randomly selected 3 points meet the resolution measurement requirement of x-axis and y-axis. When $\alpha = 1.5698$, $\beta = 0.0002$, the measured resolution of x-axis accelerometer are 11ug, 11ug and 10ug respectively, and the measured resolution of y-axis accelerometer are 11ug, 11ug and 11ug respectively; when $\alpha = 1.5708$, $\beta = -0.0002$, the measured resolution of x-axis accelerometer are 10ug, 11ug and 10ug respectively, and the measured resolution of y-axis accelerometer are 10ug, 12ug and 11ug respectively; when $\alpha = 1.5716$, $\beta = -0.001$, the measured resolution of x-axis accelerometer are 10ug, 10ug and 11ug respectively, and the measured resolution of y-axis accelerometer are 10ug, 9ug and 10ug respectively. The resolution of the tri-axial accelerometers used in this experiment are about 10ug. Considering the interference of other noises and environmental factors, there will be some errors in the measurement process. However, the difference between the experimental results and the true value are almost within 1ug, which is consistent with the theoretical derivation and simulation, demonstrating that the measurement method in this paper is feasible.

TABLE 4. Results of three repeated experiments for resolution measurement of z-axis.

Serial number	g_{ZA}(unit:g) Before rotation	After rotation	Difference
		α =0.0005 , β =0.0002	
1	0.002346	0.002335	0.000011
2	0.002348	0.002338	0.00001
3	0.002348	0.002337	0.000011
		α =0.0003 , β =0.0003	
1	0.002545	0.002534	0.000011
2	0.002545	0.002534	0.000011
3	0.002548	0.002538	0.00001
		α =0.0003 , β =-0.0004	
1	0.002555	0.002546	0.000009
2	0.002553	0.002544	0.000009
3	0.002555	0.002544	0.000011

Then the z-axis resolution measurement experiments ars carried out. Similarly, three points are randomly selected in the range of formula (18), and each point is repeated 3 times. First turn the turntable to the designated position. After the turntable is stable, rotate the frame corresponding to the axis

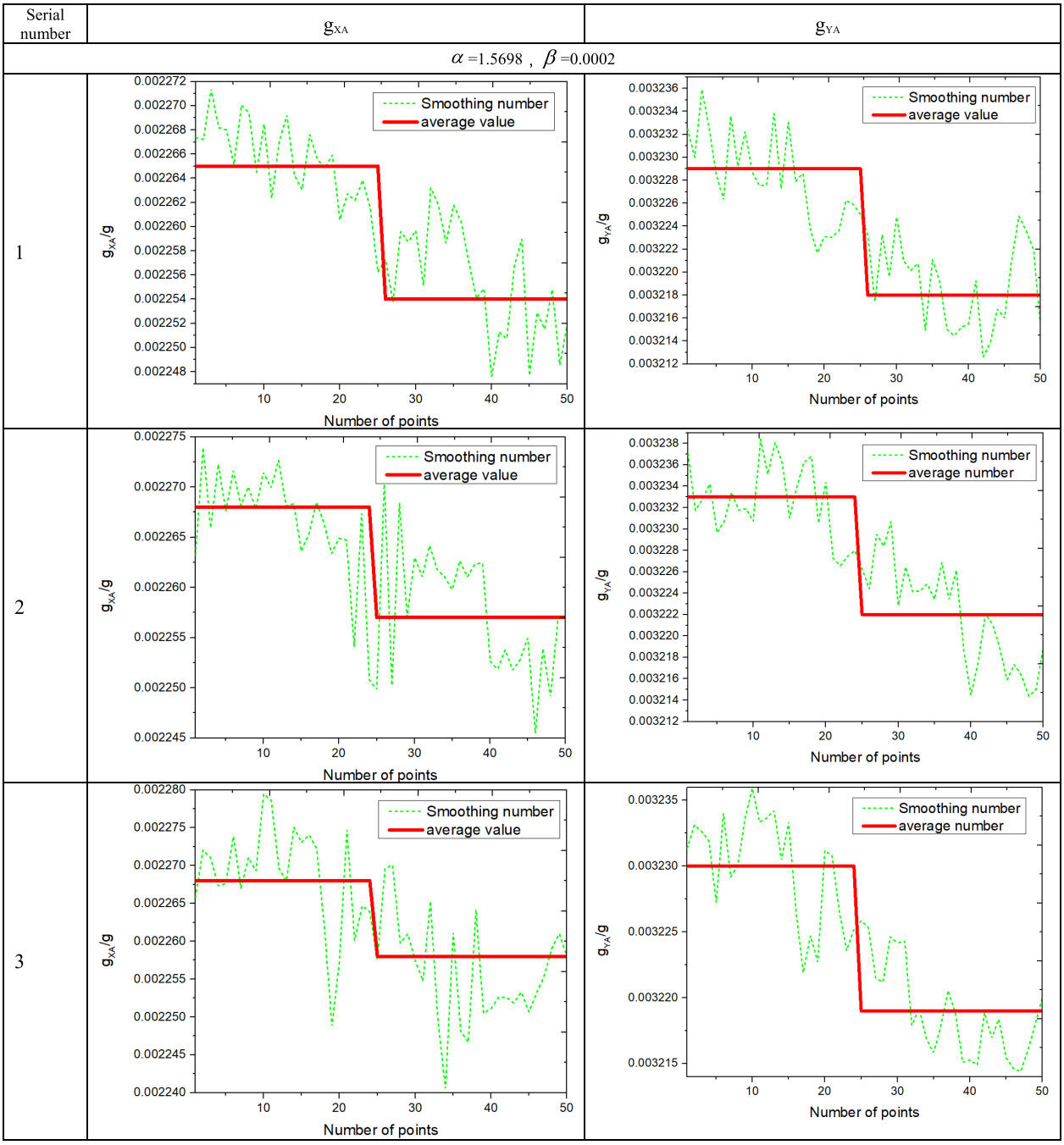

FIGURE 4. Three repeated experiments results when $\alpha = 1.5698$, $\beta = -0.0002$ for resolution measurement of X-axis and Y-axis.

TABLE 5. Results of three repeated experiments for resolution measurement process of tri-axial accelerometers.

Serial number	g_{XA}(unit:g)			g_{YA}(unit:g)			g_{ZA}(unit:g)		
	Before rotation	After rotation	Difference	Before rotation	After rotation	Difference	Before rotation	After rotation	Difference
1	0.002472	0.002462	0.000010	0.002355	0.002345	0.000010	0.002856	0.002846	0.000010
2	0.002471	0.002460	0.000011	0.002355	0.002344	0.000011	0.002856	0.002845	0.000011
3	0.002472	0.002461	0.000011	0.002354	0.002344	0.000010	0.002855	0.002845	0.000010

to be measured for 2 arc seconds, and make a difference between the data before and after rotating the turntable. The results of three repeated experiments are shown in Figure 5.

As is shown in Figure 5, there is also a tiny alteration in g_{ZA} with the rotation of turntable. The green short dash represents primary smoothing sequence. Similarly, the red

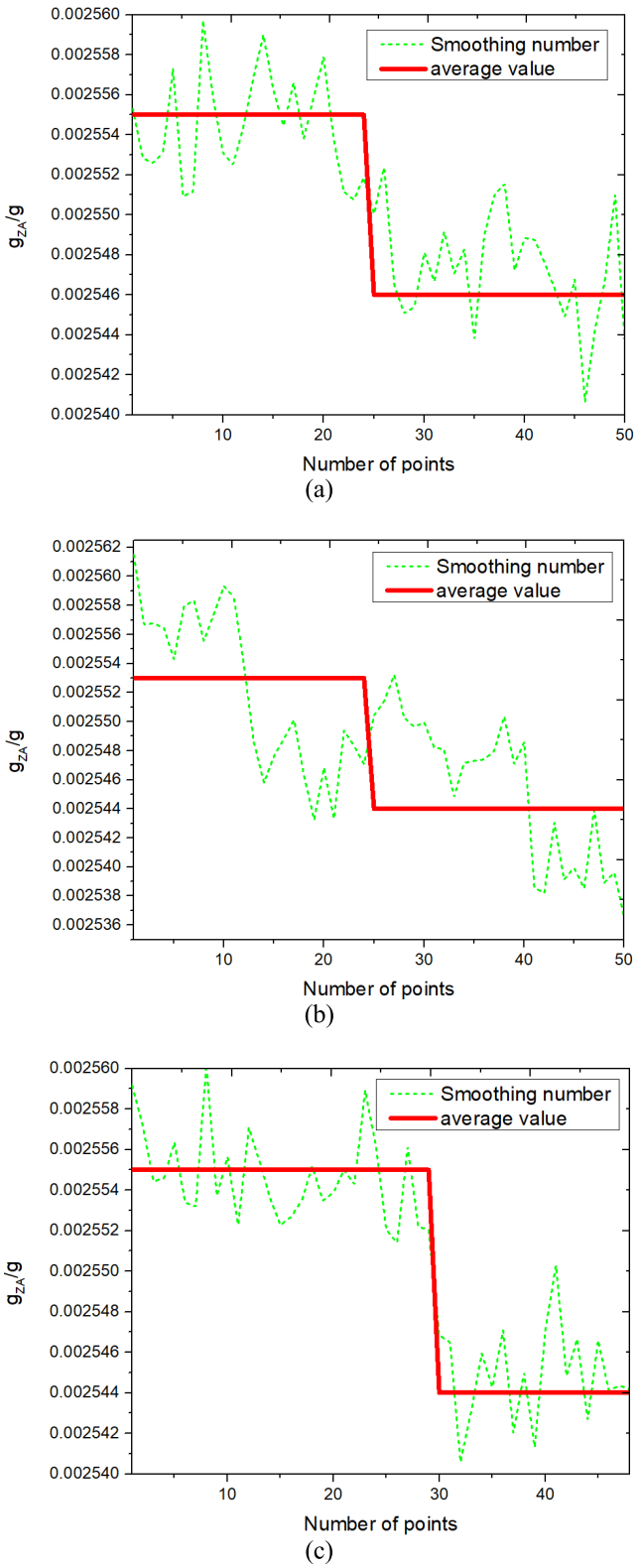

FIGURE 5. Three repeated experiments results when $\alpha = 0.0003$, $\beta = -0.0004$ for resolution measurement of Z-axis.

represent initial sequence's average value. The value of g_{ZA} are list in Table 4.

According to Table 4, the randomly selected 3 points meet the resolution measurement requirement of z-axis. When $\alpha = 0.0005$, $\beta = 0.0002$, the measured resolution of z-axis accelerometer are 11ug, 10ug and 11ug respectively; when $\alpha = 0.0003$, $\beta = 0.0003$, the measured resolution of z-axis accelerometer are 11ug, 11ug and 10ug respectively; when $\alpha = 0.0003$, $\beta = -0.0004$, the measured resolution of z-axis accelerometer are 9ug, 9ug and 11ug respectively. The resolution of the tri-axial accelerometers used in this experiment are about 10ug. However, the difference between the experimental results and the true value are almost within 1ug, which is consistent with the theoretical derivation and simulation, demonstrating that the measurement method in this paper is effective.

After the uniaxial resolution experiment, three repeated experiments are designed according to the resolution measurement process of tri-axial accelerometers in part D of Section II. First, the outer frame, inner frame and middle frame are positioned at 0 °, 0 ° and 90 ° respectively, which is the initial position for the resolution measurement. Then, the inner frame and the middle frame of the turntable are rotated for 2 arc seconds. Besides, the middle frame is rotated to 0 °, afterwards the middle frame is rotated for 2 arc seconds. Finally, the turntable is reset and closed. The results of three repeated experiments are shown in Table 5:

It can be seen from Table 5 that the designed process meets the resolution measurement conditions of tri-axial accelerometers. The results show that: the resolution of x-axis accelerometer measured by three repeated experiments are 10ug, 11ug and 11ug respectively; the resolution of y-axis accelerometer measured by three repeated experiments are 10ug, 11ug and 10ug respectively; and the resolution of z-axis accelerometer measured by three repeated experiments are 10ug, 11ug and 10ug respectively. The experimental results are consistent with the theoretical derivation and simulation, which shows that the designed process is reasonable and the method is feasible.

V. CONCLUSION

A tri-axial accelerometers resolution measurement method based on the tri-axial turntable is proposed in this paper. An rotation with small angle of the turntable is used to measure the resolution of the tri-axial accelerometers, which reduces the requirements of high-accuracy tri-axial accelerometers resolution measurement on the precision of experimental equipment. This paper mainly researches the following contents: the mathematical model of the tri-axial accelerometers resolution measurement is derived, and the general angle range that meets the measurement requirements is given. The simulation and experiment are performed within the given range. The simulation and experimental results are consistent with the theory. The process of tri-axial accelerometers resolution measurement is designed, and experiments are carried out based on the designed process. The experimental results verify the accuracy of the designed measurement process, which can provide a method reference for the tri-axial accelerometer resolutions measurement. In the next, the effect of accuracy and resolution of the experimental

set-up should be analyzed detailed and some parameters of the turntable will be added to perfect the model.

REFERENCES

[1] J. Brett and J. Brewster, "Accelerometer and rate sensor package for gravity gradiometer instruments," U.S. Patent 0 044 621, Feb. 19, 2009.
[2] J. Tie, J. Cao, L. Chang, S. Cai, M. Wu, and J. Lian, "A model of gravity vector measurement noise for estimating accelerometer bias in gravity disturbance compensation," *Sensors*, vol. 18, no. 3, pp. 883–908, Mar. 2018.
[3] L. Chang, F. Qin, and M. Wu, "Gravity disturbance compensation for inertial navigation system," *IEEE Trans. Instrum. Meas.*, vol. 68, no. 10, pp. 3751–3765, Oct. 2019.
[4] Q. He, C. Zeng, X. He, X. Xu, and Z. Lin, "Calibrating accelerometers for space-stable inertial navigation systems at system level," *Measurement*, vol. 127, pp. 472–480, Oct. 2018.
[5] Y. Li, X. J. Niu, Q. Zhang, H. P. Zhang, and C. Shi, "An *in situ* hand calibration method using a pseudo-observation scheme for low-end inertial measurement units," *Meas. Sci. Technol.*, vol. 23, no. 10, 2012, Art. no. 105104.
[6] C. Jiachong, D. Dezhi, Y. Fei, Z. Ya, and F. Shiwei, "A swing online calibration method of ship-based FOG-IMU," in *Proc. Forum Cooperat. Positioning Service (CPGPS)*, Harbin, China, May 2017, pp. 33–38.
[7] Y. Cao, H. Cai, S. Zhang, and A. Li, "A new continuous self-calibration scheme for a gimbaled inertial measurement unit," *Meas. Sci. Technol.*, vol. 23, no. 1, Jan. 2012, Art. no. 015103.
[8] B. V. Klimkovich, "SINS calibration in inertial mode. Combination of velocity and scalar methods," *Gyroscopy Navigat.*, vol. 6, no. 1, pp. 25–32, Jan. 2015.
[9] U. Qureshi and F. Golnaraghi, "An algorithm for the in-field calibration of a MEMS IMU," *IEEE Sensors J.*, vol. 17, no. 22, pp. 7479–7486, Nov. 2017.
[10] B. Li, J. Lu, W. Xiao, and T. Lin, "In-field fast calibration of FOG-based MWD IMU for horizontal drilling," *Meas. Sci. Technol.*, vol. 26, no. 3, Mar. 2015, Art. no. 035001.
[11] N. Song, Q. Cai, G. Yang, and H. Yin, "Analysis and calibration of the mounting errors between inertial measurement unit and turntable in dual-axis rotational inertial navigation system," *Meas. Sci. Technol.*, vol. 24, no. 11, Nov. 2013, Art. no. 115002.
[12] S. Ranjbaran and S. Ebadollahi, "Fast and precise solving of non-linear optimisation problem for field calibration of triaxial accelerometer," *Electron. Lett.*, vol. 54, no. 3, pp. 148–150, Feb. 2018.
[13] X. Liu, S. Wang, X. Guo, W. Yang, and G. Xu, "A method for gravitational apparent acceleration identification and accelerometer bias estimation," *IEEE Access*, vol. 7, pp. 38115–38122, Mar. 2019.
[14] S. P. Won and F. Golnaraghi, "A triaxial accelerometer calibration method using a mathematical model," *IEEE Trans. Instrum. Meas.*, vol. 59, no. 8, pp. 2144–2153, Aug. 2010.
[15] W. Guan, X. Meng, and X. Dong, "Accelerometer transverse sensitivity testing with double turntable centrifuge," in *Proc. IEEE Int. Instrum. Meas. Technol. Conf. (IMTC)*, Montevideo, Uruguay, May 2014, pp. 578–582.
[16] Q. Wu, R. Wu, F. Han, and R. Zhang, "A three-stage accelerometer self-calibration technique for space-stable inertial navigation systems," *Sensors*, vol. 18, no. 9, pp. 2888–2902, Aug. 2018.
[17] M. Yu and T. Cai, "Calibration of a rotating accelerometer gravity gradiometer using centrifugal gradients," *Rev. Sci. Instrum.*, vol. 89, no. 5, May 2018, Art. no. 054502.
[18] A. Bezděk, J. Sebera, and J. Klokocník, "Calibration of Swarm accelerometer data by GPS positioning and linear temperature correction," *Adv. Space Res.*, vol. 62, no. 2, pp. 317–325, Jul. 2018.
[19] R. D. Ma, G. L. Yang, K. Zhang, and W. Z. Zheng, "A threshold value test method for the high precision accelerometer based on twice dividing the gravitation," *Navigat. Control*, vol. 14, no. 4, pp. 110–114, Aug. 2015.
[20] W. Wu, J. X. Zhou, X. D. Liu, and L. Y. Nie, "The method for the resolution test of accelerometer based on the double axis tilt method," *Geophys. Geochem. Explor.*, vol. 39, no. S1, pp. 37–40, Dec. 2015.
[21] H. B. Li, "Dynamic estimation method for resolution of high precision accelerometer," *J. Chin. Inertial Technol.*, vol. 20, no. 4, pp. 496–500, Aug. 2012.
[22] *IEEE Recommended Practice for Precision Centrifuge Testing of Linear Accelerometers*, IEEE Standard 836, 1991.
[23] P. H. Hu, "Method for testing resolution of high-precision accelerometer for gravimeter," C.N. Patent. 1 053 343 50A, Feb. 17, 2016.

CHUNXI ZHANG received the Ph.D. degree from Zhejiang University. He is currently a Professor with the Beihang University. His current research interests are in integrated navigation and optical fiber sensing technologies.

MINPENG DAI received the bachelor's degree from Chongqing University, Chongqing, China, in 2017. He is currently pursuing the Ph.D. degree with Beihang University. His research interests are related to inertial navigation and integrated navigation.

WEI LUO received the master's degree from the School of Instrumentation and Optoelectronic Engineering, Beihang University, Beijing, China, in 2013. Since 2013, he has been working with the 9th Designing of China Aerospace Science Industry Corporation, Wuhan, China. His current research interests are integrated navigation and transfer alignment.

XIONG PAN received the Ph.D. degree from Beihang University, Beijing, China, in 2008. He is currently an Associate Professor with the Beihang University. His current research interests are in integrated navigation and inertial device.